

Novel poly-pyridyl ruthenium complexes with bis- and tris-tetrazolate mono-dentate ligands for dye sensitized solar cells†

Cite this: *RSC Adv.*, 2014, 4, 18336

Received 8th March 2014
Accepted 8th April 2014

DOI: 10.1039/c4ra02032d

www.rsc.org/advances

Tharallah A. Shoker and Tarek H. Ghaddar*

We report on a new family of ruthenium poly-pyridyl complexes that bears bis- and tris-tetrazolate mono-dentate ligands along with their spectroscopical, electrochemical, and theoretical characterization. Dye-sensitized solar cells with these complexes show good conversion efficiencies with comparable open circuit voltages to that of **N719** without the use of any additives, due to their retarded electron-recombination processes.

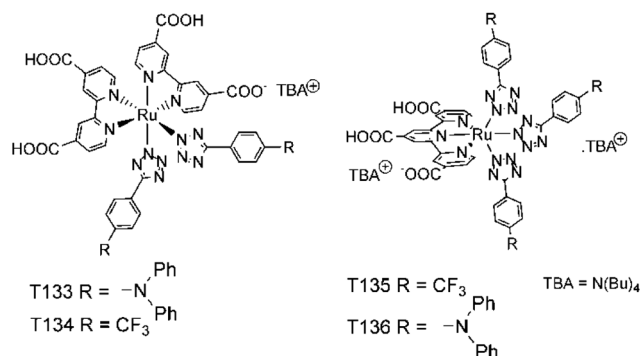
In the past two decades interest in the dye sensitized solar cell (DSSC) research area has been immense due to the DSSC's low cost of fabrication and ease of production,¹ which makes it a good candidate for commercialization. Recently, DSSC's efficiencies of 12.3% have been attained using a zinc-porphyrin complex as a sensitizer along with a liquid electrolyte system,² and efficiencies of 15% for perovskite-based solid state DSSC's.³ Up-to-date, the most commonly used dye is either the well-known N3 dye (**N719** when in the di-anionic form) [Ru(NCS)₂(dcbpy)₂] (dcbpy = 4,4'-dicarboxy-2,2'-bipyridine)⁴ or the black dye [Ru(NCS)₃(tctpy)] (tctpy = 4,4',4''-tricarboxy-2,2':6',2''-terpyridine)⁵ as very efficient sensitizers. However, designing metal based dyes that lack the thiocyanate ligand (SCN⁻), which is considered from long-term chemical stability tests as the weakest part in most ruthenium-based dyes,^{6,7} is of great interest. In addition, red-shifting the absorption band of the sensitizer in the visible and near-IR region may have positive effects on DSSCs' efficiencies.

Recently, a new class of cyclometalated complexes that lack the SCN⁻ ligand and have better light harvesting properties than **N719** has been introduced by different research groups.⁶⁻¹⁷ The high interest in this class of ruthenium based dyes is due to their good long term stability and extended absorption in the visible region (down to 800 nm). Most of this class of dyes is based on either bi- or tridentate ligands that bear either

pyrazolate, triazolate, oxyquinolate, phenyl or pyrimidinyl moieties.

In the present study, we report the design of Ru^{II} based dyes, **T133** through **T136**, that bear bis- or tris-tetrazolate mono-dentate ligands along with either two (dcbpy) or one (tctpy) moiety, respectively, Scheme 1 (see Scheme S1 ESI† for the synthetic strategy). The interesting features of these four dyes are in their chemical stability, ease of synthesis/purification and their photophysical and electrochemical properties. To our knowledge, there are no reports of ruthenium based sensitizers that bear such monodentate ligands in the literature. The four dyes were characterized by ¹H-NMR, APPI mass spectrometry, UV/vis, steady state and lifetime fluorescence measurements and electrochemistry.

In the two dyes' classes (**T133-T134** and **T135-T136**) the tetrazolate ligand bears either an electron withdrawing trifluoromethylphenyl (TFMP) group or an electron rich triphenylamine (TPA) moiety, both of which tune the redox potential of the Ru^{II} center from 1.20 to 0.89 V vs. the normal hydrogen electrode (NHE), Table 1. The presence of the electron rich TPA group would also red-shift the absorption maximum of the dye in the visible and near-IR region due to the increase in conjugation and electron donation ability. Whereas, the electron deficient TFMP group would raise the dye's redox potential



Scheme 1 Structures of the dyes T133 to T136.

American University of Beirut, PO Box: 11-0236, Beirut, Lebanon. E-mail: tarek.ghaddar@aub.edu.lb

† Electronic supplementary information (ESI) available. See DOI: 10.1039/c4ra02032d

Table 1 Spectroscopic and electrochemical data of the dyes

	λ_{abs}^a , nm (ϵ , $10^4 \text{ M}^{-1} \text{ cm}^{-1}$)	λ_{em}^b , nm (τ_{em} , ns)	$E_{1/2}$, V vs. NHE ^c	$E_{(\text{ox})}^*$, V vs. NHE
T133	311 (4.65), 380 (1.11), 513 (0.93)	715 (70)	1.35, 1.25, 1.10	-0.81
T134	311 (3.75), 380 (1.02), 508 (0.99)	705 (85)	1.20	-0.74
T135	337 (3.77), 385 (1.09), 566 (0.79)	770 (120)	1.00	-0.78
T136	333 (8.63), 388 (1.02), 572 (0.68)	767 (140)	1.35, 1.22, 0.89	-0.92
N719	306 (4.40), 379 (1.40), 525 (1.35)	755 (9)	1.08	-0.98

^a Measured in ethanol. ^b Measured in aerated ethanol with $\lambda_{\text{ex}} = 532 \text{ nm}$. ^c Measured in DMF with 0.1 M TBAPF₆.

when compared to the analogous TPA-based dye, which in turn ensures an efficient regeneration of the oxidized sensitizer by the iodide/triiodide electrolyte system upon electron injection.

The absorption and emission spectra of the four dyes in ethanol are depicted in Fig. 1. The first class of dyes (**T133**–**T134**) shows an absorption in the visible region extending down to 750 nm ($\lambda_{\text{abs}} = 513 \text{ nm}$ and 508 nm with extinction coefficients $\epsilon = 9.3$ and $9.9 \times 10^3 \text{ M}^{-1} \text{ cm}^{-1}$ for **T133** and **T134**, respectively). The **T135** and **T136** absorption extends down to 820 nm with maxima at $\lambda_{\text{abs}} = 566 \text{ nm}$ and 572 nm and extinction coefficients $\epsilon = 7.9$ and $6.8 \times 10^3 \text{ M}^{-1} \text{ cm}^{-1}$, respectively. The same trend was seen in the absorbance measurements done on 6 μm TiO₂ films dyed with the different dyes (see Fig. S4 in ESI†), suggesting that the amounts of the four different adsorbed dyes are similar. The lowest energy transitions are attributed to S₁ MLCT transitions inferred from TD-DFT calculations (see Table S1 and Fig. S2 in ESI†). The four dyes also show emission in the near-IR region, Fig. 1, with intriguing longer lifetimes than most DSSC's dyes in the literature (see Fig. S3 in the ESI†). In aerated ethanol **T133** through **T136** show emission maxima at $\lambda_{\text{em}} = 715, 705, 770$ and 767 nm and emission lifetimes of $\tau_{\text{em}} = 70, 85, 120, 140 \text{ ns}$, respectively, Fig. 1 and Table 1. Such long emission lifetimes might positively add to the enhancement of electron injection efficiency.

The electrochemical properties of the different ruthenium complexes (**T133** through **T136**) were evaluated by differential pulse voltammetry in dimethylformamide (DMF), Fig. 2 (see also Fig. S1 in the ESI†). The Ru^{II/III} redox potentials of the four dyes were measured to be $E_{1/2} = 1.10, 1.20, 1.00$ and 0.89 vs.

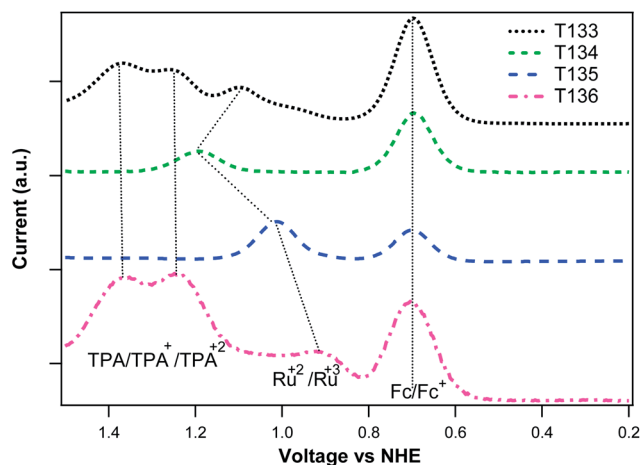


Fig. 2 Differential pulse voltammograms (0.1 M Bu₄NPF₆, DMF) for **T133** to **T136**.

NHE for **T133** through **T136**, respectively), Table 1. **T134** and **T135** showed only one redox peak between 0.2 and 1.5 V which is attributed to the oxidation/reduction of the Ru^{II/III} center. Upon comparing the redox potentials of the four dyes shows that upon the introduction of a third tetrazolate ligand a shift of $\sim 0.2 \text{ V}$ is seen for **T135** and **T136** when compared to **T134** and **T133**, respectively. As expected, **T134** had the highest potential due to the electron withdrawing effect of the TFMP group on the ruthenium center. **T133** and **T136** show in addition to the ruthenium's redox potential two redox peaks in the scanned potential window which are attributed to the redox active TPA groups.

The derived redox potentials of the dyes' excited states from both the Ru^{II/III} redox potential and the optical energy gap (E_{0-0} was calculated from the intersection of the lowest energy MLCT band and the emission band) ranges between $E_{(\text{ox})}^* = -0.74$ and -0.92 V vs. NHE. These values are higher than that of the TiO₂ conduction band edge (CB) (-0.5 V vs. NHE), and thus upon photo excitation of these complexes fast and efficient electron injection into the TiO₂ CB is expected.

DSSCs employing a 12 μm thick TiO₂ layer plus a 4 μm scattering layer (300 nm) were fabricated using the four different dyes in addition to a DSSC employing the **N719** dye for comparison. The TiO₂ films were stained by the respective dye solution (0.3 mM) in ethanol for 18 h without any additives. An electrolyte solution (EL1) made of 0.6 M 1,2-dimethyl-3-propylimidazolium

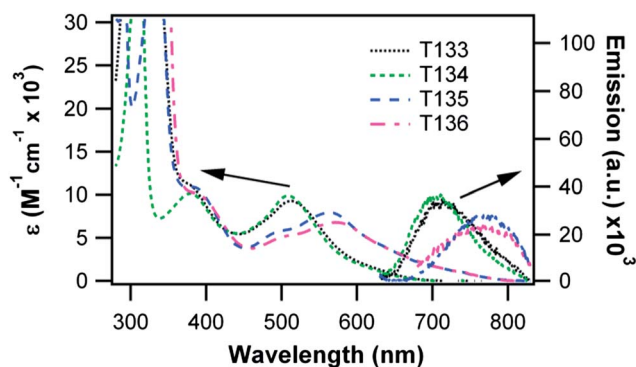


Fig. 1 Absorption and emission spectra ($\lambda_{\text{ex}} = 532 \text{ nm}$) of **T133** (dotted – black), **T134** (dashed – green), **T135** (dashed-dotted – blue) and **T136** (dashed-dotted-dotted – violet) in ethanol.

iodide (MPlI), 0.1 M guanidinium thiocyanate (GuNCS), 0.05 M LiI, 0.03 M I₂ and 0.5 M 4-*tert*-butylpyridine (TBP), in methoxypropanonitrile (MPN), was used in these studies. The photocurrent *vs.* voltage (*I*-*V*) responses of the above mentioned cells are shown in Fig. 3 and summarized in Table 2. The lower fill factors (FF) and open circuit voltages (*V*_{oc}) of the studied cells when compared to values in the literature are mainly due to the geometry of the cells studied (1 × 1 cm). The T133 through T136 based cells afforded good performances except for T136, with short-circuit photocurrents *J*_{sc} = 13.1, 12.0, 13.0 and 6.7 mA cm⁻², *V*_{oc} = 620, 620, 622 and 495 mV, FF = 0.65, 0.67, 0.66 and 0.65 and efficiencies η = 5.3, 5.0, 5.3 and 2.2%, respectively, under simulated AM1.5G solar illumination at 100 mW cm⁻². In the case of N719, the cell showed a slightly higher performance with *J*_{sc} = 14.6 mA cm⁻², *V*_{oc} = 637 mV, FF = 0.67 and η = 6.2%.

The measured incident photon to electron conversion efficiency (IPCE) spectra of the T133 through T136 and N719 based cells are shown in Fig. 4. As can be seen, T133 and T134 show similar IPCE values to N719 but blue shifted by 20 and 25 nm, respectively, which is consistent with their UV/vis spectra. From the IPCE, integrated current and *I*-*V* measurements one can conclude that T133 and T134 show similar electron injection and dye regeneration to N719.

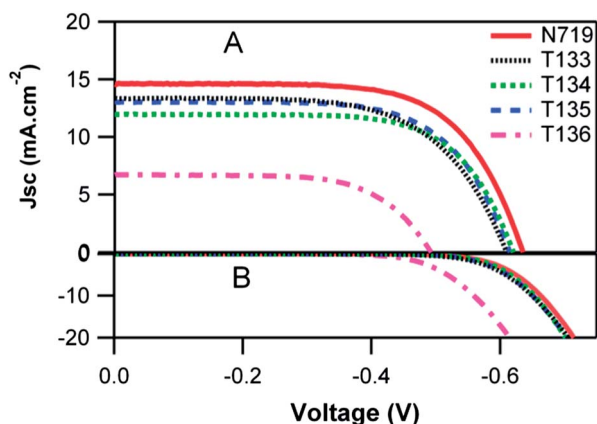


Fig. 3 (A) Photocurrent–voltage characteristics of DSSCs sensitized with dyes: N719 (solid – red) and T133 (dotted – black), T134 (dashed – green), T135 (dashed-dotted – blue) and T136 (dashed-dotted-dotted – violet) with electrolyte EL1. (B) Dark currents of the corresponding cells.

Table 2 DSSCs' performance of T133 through T136 and N719 dyes

	<i>J</i> _{sc} , mA cm ⁻²	<i>V</i> _{oc} , mV	FF	η^a (%)
T133	13.1	620	0.65	5.3
T134	12.0	620	0.67	5.0
T135	13.0	622	0.66	5.3
T136	6.7	495	0.65	2.2
N719	14.6	637	0.67	6.2

^a Measured under 100 mW cm⁻² simulated AM1.5 spectrum with an active area = 0.126 cm². Electrolyte EL1: 0.6 M DMPII, 0.05 M LiI, 0.5 M TBP, 0.1 M GuSCN and 0.03 M I₂ in MPN.

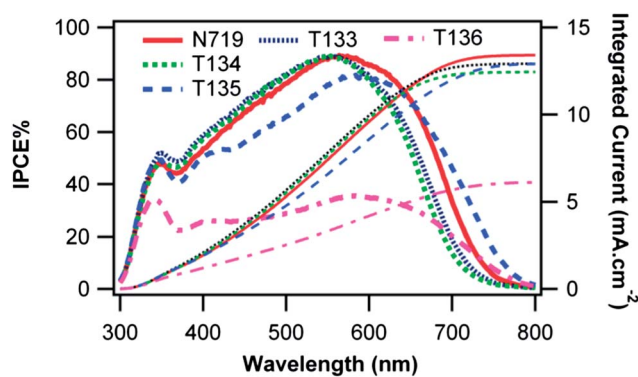


Fig. 4 IPCE% and integrated current spectra of N719 (solid – red) and T133 (dotted – black), T134 (dashed – green), T135 (dashed-dotted – blue) and T136 (dashed-dotted-dotted – violet) assembled cells with electrolyte EL1.

Moreover, the higher *J*_{sc} value shown by T133 when compared to T134 is mainly attributed to the former's better light absorption (5 nm red shift). As for T135, the IPCE spectrum shows lower IPCE% values but red shifted by ~20 nm when compared to N719. When using EL1 as the electrolyte system, T136 shows much lower IPCE% values than N719 with a similar red shift as T135 (this will be discussed at a later stage). The IPCE spectrum of T135 highlights the better absorption nature of T135 than N719 in the near-IR, however, the measured lower photo-current of T135 could be attributed to its lower absorption extinction coefficient.

In order to understand the above mentioned results (lower efficiency of T136 than N719), we performed electrochemical impedance spectroscopy (EIS) measurements on the five different assembled cells at *V*_{oc} under different light intensities. EIS spectra were analyzed using an established equivalent-circuit that interprets the different interfaces in a DSSC through a transmission line model.^{18,19} Fig. 5 shows a plot of the chemical capacitance values at the TiO₂–electrolyte interface (*C*_μ), for the different cells extracted from the EIS experiments, *versus* the corrected applied voltage (*nE*_F – *E*_{F,redox})_{cor.}, where *nE*_F is the electron quasi-Fermi energy level in the TiO₂ film and

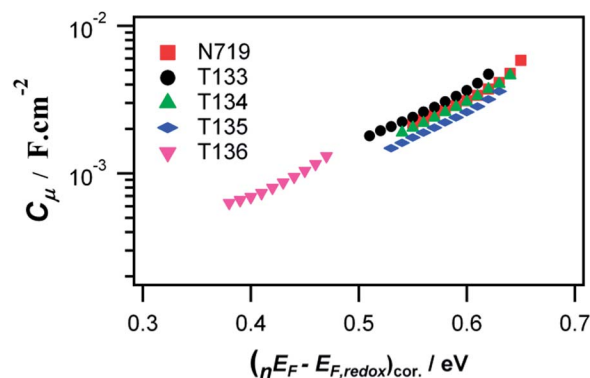


Fig. 5 Capacitance values obtained from EIS of N719 (square – red) and T133 (circle – black), T134 (triangle – green), T135 (rhombus – blue) and T136 (triangle – violet) assembled cells with electrolyte EL1.

$E_{F,redox}$ is the electrolyte redox Fermi level, (the applied voltage is corrected for voltage drop due to the total series resistance,²⁰ R_s). The C_{μ} values for the five cells show an exponential behavior as a function of the corrected applied voltage, where this is due to the trap energy distribution below the conduction band edge.²¹

Considering that the five different cells have the same trap energy distribution (since the TiO_2 film is identical in all cells) and the same electrolyte solution is used in these cells, the observed shifts in the $(nE_F - E_{F,redox})_{cor.}$ towards higher or lower values could be attributed to an upward or downward shifts in the conduction band edge, respectively.^{22,23} The observed shifts $\Delta(nE_F - E_{F,redox})_{cor.}$ compared to **N719** lies between +10 and -10 mV for the four tetrazolate based dyes, Fig. 5, which is within our experimental data errors. As such, we can assume that there is no significant shift in the conduction band edge in the five different cells. However, the plots of the charge recombination resistance at the TiO_2 -electrolyte interface (R_{ct}) versus $(nE_F - E_{F,redox})_{cor.}$ show some differences between the five DSSCs, Fig. 6. DSSCs that incorporate **T133** through **T135** show slightly smaller R_{ct} values than **N719** (where a smaller R_{ct} value indicates faster electron recombination from the TiO_2 to the electrolyte solution or oxidized dye, and thus lower V_{oc} values). However, the **T136** based DSSC shows much smaller R_{ct} values than **N719**, which suggests fast electron recombination processes at the dyed TiO_2 -electrolyte interface and in turn causes the low V_{oc} value of 495 mV. These results are also consistent with the dark currents measured for the respective cells, Fig. 3B.

Open circuit voltage decay (OCVD) experiments were conducted to probe the electron recombination processes. Fig. 7 shows the effective electron lifetime (τ_n) obtained from OCVD measurements,²⁴ in addition to the τ_n values derived from the EIS experiments (from EIS $\tau_n = R_{ct}C_{\mu}$). Electron lifetimes obtained from the two different techniques (OCVD and EIS) are in good agreement. The τ_n values for the **T133** through **T135** based cells are only ~ 1.7 times shorter than that of **N719**. However, **T136**, and as inferred by all of the performed measurements, shows a much shorter τ_n than **N719** by ~ 52 times.

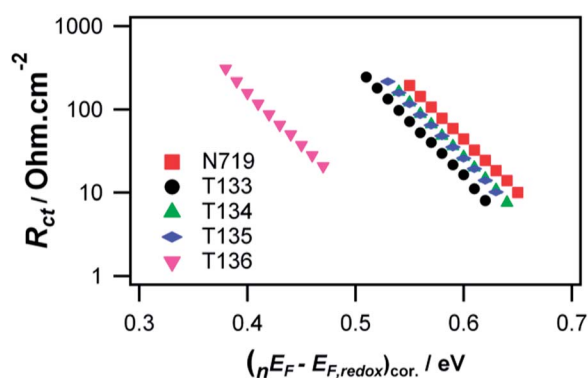


Fig. 6 Charge transfer resistance values obtained from EIS of **N719** (square – red) and **T133** (circle – black), **T134** (triangle – green), **T135** (rhombus – blue) and **T136** (triangle – violet) assembled cells with electrolyte EL1.

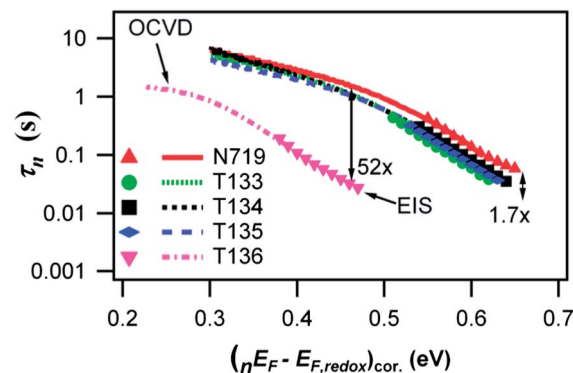


Fig. 7 Electron lifetimes obtained from OCVD and EIS of **N719** (square – red) and **T133** (circle – black), **T134** (triangle – green), **T135** (rhombus – blue) and **T136** (triangle – violet) assembled cells with electrolyte EL1.

Therefore, the slight lower performance of **T133** to **T135** than **N719** is due to the blue-shift in the absorption spectra of **T133** and **T134** and slightly faster electron recombination processes, whereas that of **T135** is due to the latter reason and its low absorption extinction coefficient. However, the much lower efficiency of **T136** when compared to **T133**–**T135** and **N719** is mainly due to accelerated electron recombination processes. The accumulated electrons in the TiO_2 can either recombine with the oxidized dye upon electron injection or to the electrolyte system. The former mechanism becomes significant when the oxidized dye is not sufficiently regenerated by the electrolyte redox system.²⁵ In addition, the dye structure can have profound effects on the electron recombination processes, where it was shown by different research groups that depending on the molecular structure of the dye binding to iodine²⁶ or even iodide²⁷ can take place and affects the DSSC performance negatively or positively, respectively. In order to pinpoint the reason behind such increased electron recombination kinetics in the case of **T136**, we used a different electrolyte system (EL2: 2.0 M 1,3-dimethylimidazolium iodide (DMII), 0.1 M GuNCS, 0.05 M LiI, 0.03 M I_2 and 0.5 M TBP in MPN) that we and other

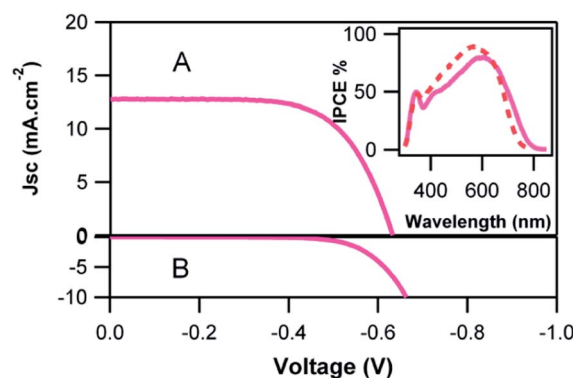


Fig. 8 (A) Photocurrent–voltage characteristics of **T136** DSSC with EL2 as the electrolyte system; (inset) IPCE spectra of **N719** (dashed – red) and **T136** (solid – violet) using EL2. (B) Dark current of the corresponding **T136** cell.

groups⁴⁴ use with dyes that possess redox potentials below 1.0 eV vs. NHE and might be inefficiently regenerated with electrolyte systems with low iodide concentrations such as in EL1. Indeed, with EL2 (compared to EL1) **T136** shows an increase in efficiency from 2.2% to 5.3% with higher values of $J_{sc} = 12.8 \text{ mA cm}^{-2}$ and $V_{oc} = 630 \text{ mV}$ than that with EL1, Fig. 8.

In addition, **T136** shows a comparable electron lifetime to the other dyes when EL2 is used as the corresponding electrolyte, (see Fig. S5 in the ESI†). Therefore, it would be safe to conclude that in the case of **T136** the lower performance shown with EL1 than with EL2 might be due to an inefficiency in its regeneration by EL1. However, at this point one cannot be sure if this is due to **T136** lower redox potential than the other three dyes or to its different molecular structure when anchored on TiO_2 .

Conclusions

In summary, we have successfully designed and synthesized a new class of ruthenium based dyes using bis- and tris-tetrazolate ligands that show interesting photophysical and electrochemical properties. Good DSSCs efficiencies were attained with these new dyes and will surely be improved in the near future, and the achievement of comparable efficiencies to the **N719** cells is remarkable for this first new family of dyes. We are currently designing similar dyes with long aliphatic chains and increased conjugation. Using long aliphatic chains, on such more manipulative ligands than a thiocyanate is, would decrease electron recombination processes.^{28,29} Whereas extending the conjugation in these ligands might increase the absorption extinction coefficient and thus attain better light harvesting ability.

Acknowledgements

This work was supported by the University Research Board (URB) at the American University of Beirut (AUB) and the Lebanese National Council for Scientific Research (LNCRSR).

Notes and references

- B. O'Regan and M. Grätzel, *Nature*, 1991, **353**, 737–740.
- A. Yella, H.-W. Lee, H. N. Tsao, C. Yi, A. K. Chandiran, M. K. Nazeeruddin, E. W.-G. Diao, C.-Y. Yeh, S. M. Zakeeruddin and M. Grätzel, *Science*, 2011, **334**, 629–634.
- J. Burschka, N. Pellet, S.-J. Moon, R. Humphry-Baker, P. Gao, M. K. Nazeeruddin and M. Grätzel, *Nature*, 2013, **499**, 316–319.
- M. K. Nazeeruddin, F. De Angelis, S. Fantacci, A. Selloni, G. Viscardi, P. Liska, S. Ito, B. Takeru and M. Grätzel, *J. Am. Chem. Soc.*, 2005, **127**, 16835–16847.
- M. K. Nazeeruddin, P. Pechy, T. Renouard, S. M. Zakeeruddin, R. Humphry-Baker, P. Comte, P. Liska, L. Cevey, E. Costa, V. Shklover, L. Spiccia, G. B. Deacon, C. A. Bignozzi and M. Grätzel, *J. Am. Chem. Soc.*, 2001, **123**, 1613–1624.
- T. Bessho, E. Yoneda, J.-H. Yum, M. Guglielmi, I. Tavernelli, H. Imai, U. Rothlisberger, M. K. Nazeeruddin and M. Grätzel, *J. Am. Chem. Soc.*, 2009, **131**, 5930–5934.
- M. Grätzel, *Acc. Chem. Res.*, 2009, **42**, 1788–1798.
- T. Funaki, M. Yanagida, N. Onozawa-Komatsuzaki, K. Kasuga, Y. Kawanishi, M. Kurashige, K. Sayama and H. Sugihara, *Inorg. Chem. Commun.*, 2009, **12**, 842–845.
- H. Kisserwan and T. H. Ghaddar, *Dalton Trans.*, 2011, **40**, 3877–3884.
- K. C. D. Robson, B. D. Koivisto, A. Yella, B. Spornova, M. K. Nazeeruddin, T. Baumgartner, M. Grätzel and C. P. Berlinguette, *Inorg. Chem.*, 2011, **50**, 5494–5508.
- P. G. Bomben, K. C. D. Robson, B. D. Koivisto and C. P. Berlinguette, *Coord. Chem. Rev.*, 2012, **256**, 1438–1450.
- K.-L. Wu, S.-T. Ho, C.-C. Chou, Y.-C. Chang, H.-A. Pan, Y. Chi and P.-T. Chou, *Angew. Chem., Int. Ed.*, 2012, **51**, 5642–5646.
- C.-C. Chou, K.-L. Wu, Y. Chi, W.-P. Hu, S. J. Yu, G.-H. Lee, C.-L. Lin and P.-T. Chou, *Angew. Chem., Int. Ed.*, 2011, **50**, 2054–2058.
- C.-W. Hsu, S.-T. Ho, K.-L. Wu, Y. Chi, S.-H. Liu and P.-T. Chou, *Energy Environ. Sci.*, 2012, **5**, 7549–7554.
- T. Funaki, H. Funakoshi, O. Kitao, N. Onozawa-Komatsuzaki, K. Kasuga, K. Sayama and H. Sugihara, *Angew. Chem., Int. Ed.*, 2012, **51**, 7528–7531.
- H. C. Zhao, J. P. Harney, Y.-T. Huang, J.-H. Yum, M. K. Nazeeruddin, M. Grätzel, M.-K. Tsai and J. Rochford, *J. Inorg. Chem.*, 2012, **51**, 51.
- B. Schulze, D. G. Brown, K. C. D. Robson, C. Friebe, M. Jäger, E. Birekner, C. P. Berlinguette and U. S. Schubert, *Chem. –Eur. J.*, 2013, **19**, 1521–3765.
- Q. Wang, S. Ito, M. Grätzel, F. Fabregat-Santiago, I. n. Mora-Seró, J. Bisquert, T. Bessho and H. Imai, *J. Phys. Chem. B*, 2006, **110**, 25210–25221.
- F. Fabregat-Santiago, G. Garcia-Belmonte, I. Mora-Sero and J. Bisquert, *Phys. Chem. Chem. Phys.*, 2011, **13**, 9083–9118.
- T. Stergiopoulos, M. Konstantakou and P. Falaras, *RSC Adv.*, 2013, **3**, 15014–15021.
- J. Bisquert, *Phys. Chem. Chem. Phys.*, 2003, **5**, 5360–5364.
- V. González-Pedro, X. Xu, I. n. Mora-Seró and J. Bisquert, *ACS Nano*, 2010, **4**, 5783–5790.
- E. Guillén, L. M. Peter and J. A. Anta, *J. Phys. Chem. C*, 2011, **115**, 22622–22632.
- A. Zaban, M. Greenshtein and J. Bisquert, *ChemPhysChem*, 2003, **4**, 859–864.
- K. C. D. Robson, K. Hu, G. J. Meyer and C. P. Berlinguette, *J. Am. Chem. Soc.*, 2013, **135**, 1961–1971.
- X. Li, A. Reynal, P. Barnes, R. Humphry-Baker, S. M. Zakeeruddin, F. De Angelis and B. C. O'Regan, *Phys. Chem. Chem. Phys.*, 2012, **14**, 15421–15428.
- J. Jeon, W. A. Goddard and H. Kim, *J. Am. Chem. Soc.*, 2013, **135**, 2431–2434.
- L. Schmidt-Mende, J. E. Kroeze, J. R. Durrant, M. K. Nazeeruddin and M. Grätzel, *Nano Lett.*, 2005, **5**, 1315–1320.
- S. M. Zakeeruddin, M. K. Nazeeruddin, R. Humphry-Baker, P. Pechy, P. Quagliotto, C. Barolo, G. Viscardi and M. Grätzel, *Langmuir*, 2002, **18**, 952–954.